

Interpretable Image Classification with Differentiable Prototypes Assignment

Dawid Rymarczyk^{1,2}Łukasz Struski¹Michał Górszczak¹Koryna Lewandowska³Jacek Tabor¹Bartosz Zieliński^{1,2}¹ Faculty of Mathematics and Computer Science, Jagiellonian University² Ardigen SA³ Department of Cognitive Neuroscience and Neuroergonomics, Institute of Applied Psychology, Jagiellonian University

Abstract

We introduce *ProtoPool*, an interpretable image classification model with a pool of prototypes shared by the classes. The training is more straightforward than in the existing methods because it does not require the pruning stage. It is obtained by introducing a fully differentiable assignment of prototypes to particular classes. Moreover, we introduce a novel focal similarity function to focus the model on the rare foreground features. We show that *ProtoPool* obtains state-of-the-art accuracy on the CUB-200-2011 and the Stanford Cars datasets, substantially reducing the number of prototypes. We provide a theoretical analysis of the method and a user study to show that our prototypes are more distinctive than those obtained with competitive methods. We made the code available.

1. Introduction

The broad application of deep learning in fields like medical diagnosis [3] and autonomous driving [59], together with current law requirements (i.e. GDPR in EU [24]), enforces models to explain the rationale behind their decisions. That is why explainers [6, 26, 33, 44, 49] and self-explainable [4, 7, 63] models are developed to justify neural network outputs. Some of them are inspired by mechanisms used by humans to explain their decisions, like matching image parts with memorized prototypical features that an object poses [8, 31, 39, 48].

Recently, Prototypical Part Network (ProtoPNet) [8] was introduced, employing feature matching learning theory [45, 46]. It focuses on crucial image parts and compares them with a reference pattern (prototypical part) assigned to a class. The comparison is based on a similarity metric between the image activation map and representations of

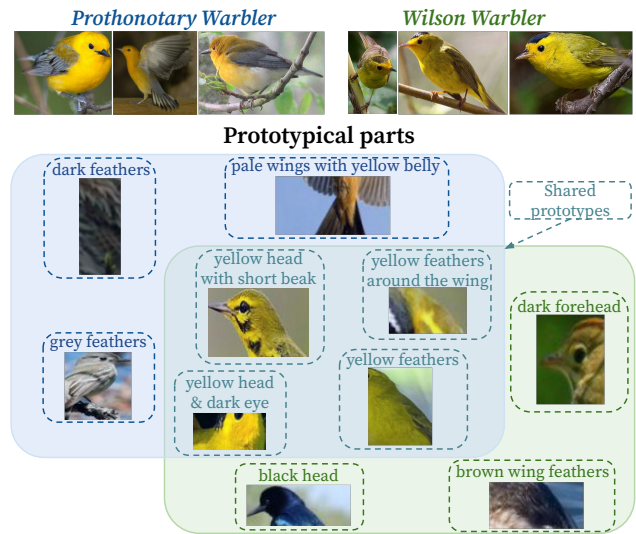


Figure 1. Automatically discovered prototypes¹ shared between two classes (*Prothonotary Warbler* and *Wilson Warbler*, each represented by 3 images). 3 prototypical parts on the blue and green background are specific for a *Prothonotary Warbler* and *Wilson Warbler*, respectively. While 4 prototypes shared between those classes are presented as the intersection. One can observe that *ProtoPool* shares prototypes related to yellow feathers of the *Warblers* between those two classes and identifies birds' heads and wing feathers as differentiating features. Prototypes sharing reduces their amount, leads to a more interpretable model, and allows to discover similarities between classes.

prototypical parts (later called prototypes). The maximum value of similarity is pooled to the classification layer.

However, ProtoPNet assumes that each class has its own separate set of prototypes, which is problematic because many object features can repeat through many classes. For instance, both *Prothonotary Warbler* and *Wilson Warbler* have yellow feathers (see Figure 1). Such limitation of ProtoPNet hinders the scalability because it means the linear growth of prototypes with the growing number of classes.

¹Names of prototypical parts are provided by the authors.

This highly increases the number of prototypes, making ProtoPNet harder to interpret by the users. Moreover, many of ProtoPNet’s prototypes correspond to the background [48].

To address these limitations, ProtoPShare [48] and ProtoTree [39] were introduced, reducing the number of prototypical parts by sharing them between classes. However, ProtoPShare requires previously trained ProtoPNet to perform the merge-pruning step, which extends the training time. At the same time, ProtoTree builds a decision tree and exploits the negative reasoning process. This, on the other hand, may result in an explanation containing no positive matches, which are difficult to comprehend. For example, a model can predict a *sparrow* because it lacks red feathers, long beak, and wide wings. Finally, other methods like TCAV [26] and Concept Whitening [9] require a predefined concept dictionary to learn and present the explanation.

To deal with the above mentioned shortcomings, in this paper we introduce ProtoPool, a self-explainable prototype model for fine-grained images classification. In ProtoPool, we implement a few major novel elements that substantially reduce the number of prototypes compared to the previous models like ProtoPNet, ProtoPShare, and ProtoTree, while obtaining higher interpretability and easier training. Instead of using hard assignment of prototypes to classes, we implement the soft prototypes given as a distribution over the set of prototypes. This distribution is randomly initialized and binarized during training with the use of the Gumbel-Softmax trick. This mechanism simplified the training process by removing the pruning step required in ProtoPNet, ProtoPShare, and ProtoTree. The second novelty is a focal similarity function that focuses the model on the rare foreground features. For this purpose, instead of maximizing the global activation, we maximize the gap between the maximum and mean similarity between the image activation map and prototypes (see Figure 2). As a consequence, we obtain strongly localized prototypes which, as shown in user study (see Figure 10), are more interpretable than those obtained with the other prototypical models.

We confirm the effectiveness of ProtoPool with theoretical analysis and exhaustive experiments, showing that it achieves the highest accuracy among models with a reduced number of prototypes. What is more, we discuss interpretability, perform a user study, and discuss the cognitive aspects of the ProtoPool over existing methods.

The main achievements of the paper can be summarized as follows:

- We construct ProtoPool, a case-based self-explainable method that shares prototypes between data classes without any predefined concept dictionary.
- We introduce fully differentiable assignments of prototypes to classes, allowing the end-to-end training.
- We define a novel similarity function, called focal sim-

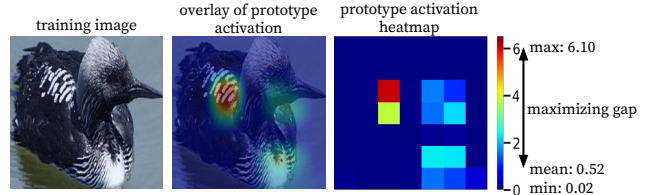


Figure 2. Automatically derived prototypes may ignore the foreground and focus on the background with very general features. As the background is usually uniform, this results in many high values in the activation map. To prevent that, we introduce a focal similarity that maximizes the gap between the maximum and the mean value of prototype activation. This way, we generate prototypes that concentrate on the rare foreground elements corresponding to only one high value in the activation map. In the presented image, the maximum activation is at the wing with white-black stripes, while the other activation values are suppressed.

ilarity, that focuses the model on the rare foreground elements.

- We increase interpretability by reducing prototypes number and providing explanations in a positive reasoning process.

2. Related works

Attempts to explain deep learning models can be divided into the post hoc and self-explainable [47] methods. The former assume that the reasoning process is hidden in a black box model and create an explainer model to reveal it. This type of methods includes a saliency map [35, 43, 49–51] that generates a heatmap of crucial image parts. Another technique is Concept Activation Vectors (CAV), explaining the internal network state as user-friendly concepts [9, 16, 26, 29, 61]. Other methods analyze the networks’ reaction to the image perturbation [6, 13, 14, 44] or provide counterfactual examples [1, 17, 37, 41, 58]. Post hoc methods are easy to implement because they do not interfere with the architecture, but they can produce biased and unreliable explanations [2]. That is why more focus is recently put on designing self-explainable models [4, 7] to make the decision process directly visible. Many interpretable solutions are based on the attention [32, 53, 60, 62–64] or exploit the activation space [18, 42], e.g. with adversarial auto-encoder. Finally, a very popular interpretable method introduced in [8] (ProtoPNet) has a hidden layer of prototypes representing the activation patterns.

ProtoPNet was extended since its publication, e.g. by TesNet [57] that constructs the latent space on a Grassman manifold without prototypes reduction. Alternatively, models like ProtoPShare [48] and ProtoTree [39] reduce the number of prototypes used in the classification. The ProtoPShare introduces data-dependent merge-pruning that discovers prototypes of similar semantics and joins them.

While the ProtoTree uses a soft neural decision tree that depends also on the negative reasoning process. Approaches similar to ProtoPNet organize the prototypes hierarchically [19] to classify input at every level of a predefined taxonomy or transform prototypes from the latent space to data space [31]. Lastly, prototype-based solutions are widely adopted in various fields like medical imaging [3, 5, 27, 52], time series analysis [15], and sequence learning [36].

3. ProtoPool

In this section, we first describe the overall architecture of ProtoPool presented in Figure 3, and then we provide its crucial details. We concentrate on describing the main novelties of ProtoPool compared to the existing models, such as assigning pool prototypes to classes and modifying the similarity function. Finally, we provide a theoretical analysis of ProtoPool.

Overall architecture The architecture of ProtoPool, shown in Figure 3, is generally inspired by ProtoNet [8]. It consists of convolutional layers f , a prototype pool layer g , and a fully connected layer h . Layer g contains a pool of M trainable prototypes $P = \{p_i \in \mathbb{R}^D\}_{i=1}^M$ and K slots for each class. Each slot is implemented as a distribution $q_k \in \mathbb{R}^M$ of prototypes available in the pool, where successive values of q_k correspond to the probability of assigning successive prototypes to slot k , and $\|q_k\| = 1$.

Given an input image $x \in X$, the convolutional layers first extract image representation $f(x)$ of shape $H \times W \times D$. Intuitively, $f(x)$ can be considered as a set of $H \cdot W$ vectors of dimension D , each corresponding to specific location of the image (as presented in Figure 3). For the clarity of description, we will denote this set as $Z_x = \{z_i \in f(x) : z_i \in \mathbb{R}^D, i = 1..H \cdot W\}$. Then, ProtoPool computes the similarity $g(Z_x, q)$ between Z_x and each distribution q using the prototype pool layer. Finally, the similarity scores (K values per class) are multiplied by the weight matrix w_h in the fully connected layer h . This results in the output logits that are normalized using softmax to obtain a final prediction.

Assigning one prototype per slot Previous prototypical methods use the hard assignment of the prototypes to classes [8, 48, 57] or nodes of a tree [39]. Therefore, no gradient propagation is needed to model the prototypes assignment. In contrast, our ProtoPool uses a soft assignment based on prototypes’ distributions to optimally use prototypes from the pool. To generate prototype distribution q , one could apply softmax on the vector of size \mathbb{R}^M . However, this could result in assigning many prototypes to one slot, consequently decreasing the interpretability. Therefore, to obtain probability close to 1 for exactly one prototype, we require a differentiable arg max function. A perfect match, in this case, seems to be the Gumbel-Softmax estimator [23], where for $q = (q^1, \dots, q^M) \in \mathbb{R}^M$ and

$\tau \in (0, \infty)$

$$\text{Gumbel-softmax}(q, \tau) = (y^1, \dots, y^M) \in \mathbb{R}^M,$$

where $y^i = \frac{\exp((q^i + \eta_i)/\tau)}{\sum_{m=1}^M \exp((q^m + \eta_m)/\tau)}$ and η_m for $m \in 1, \dots, M$ are samples drawn from standard Gumbel distribution. The Gumbel-Softmax distribution interpolates between continuous categorical densities and discrete one-hot-encoded categorical distributions, approaching the latter for low temperatures $\tau \in [0.1, 0.5]$ (see Figure 4).

Slots’ orthogonality The same prototype can be assigned to many class slots, wasting the capacity of the prototype pool layer and returning poor results. That is why we extended the loss function with

$$\mathcal{L}_{orth} = \sum_{i < j}^K \frac{\langle q_i, q_j \rangle}{\|q_i\|_2 \cdot \|q_j\|_2}, \quad (1)$$

where q_1, \dots, q_K are the distributions of a particular class. As a result, successive slots of a class are assigned to different prototypes.

Focal similarity In the standard ProtoPNet approach [8], also used by its extensions, the similarity function of two points p and z in the representation space is given by²

$$g(z, p) = \log\left(1 + \frac{1}{\|z-p\|^2}\right) \in [0, \infty).$$

Let us recall that given an input image x , its representation $f(x)$ can be considered as a set of $H \cdot W$ vectors of dimension D , denoted as $Z_x = \{z \in f(x)\}$. Thus in ProtoPNet, the final activation of the prototype p with respect to image x is given by

$$g_{\max}(Z_x, p) = \max_{z \in Z_x} g(z, p).$$

One can observe that such an approach has two possible disadvantages. First, high activation can also be obtained when all the elements in Z_x have a high similarity to the prototype. It is unfavorable, as it means that prototypes can concentrate on the image background. The other negative aspect concerns the training process, as using max means that the gradient is passed only through the most active part of the image.

To prevent such unwanted behaviors, in ProtoPool, we introduce a novel similarity function that contrasts max with the mean activation

$$g_{\text{focal}}(Z_x, p) = \max_{z \in Z_x} g(z, p) - \text{mean}_{z \in Z_x} g(z, p). \quad (2)$$

This implies that the maximal activation happens if only one part of the image x (i.e. the corresponding pixel in representation space) is similar to the prototype (see Figure 2). Consequently, the constructed prototypes correspond to rare foreground features, and the gradient passes through all elements of Z_x . To finalize description of our method, we generalize this mechanism to distribution over the set of prototypes P by taking the expected value. Naturally, for a degenerated distribution concentrated at a prototype, we obtain the same formula as for the hard assignment.

²The following regularization is used to avoid the numerical instability in the experiments: $g(z, p) = \log\left(\frac{\|z-p\|^2 + 1}{\|z-p\|^2 + \epsilon}\right)$, with a small $\epsilon > 0$.

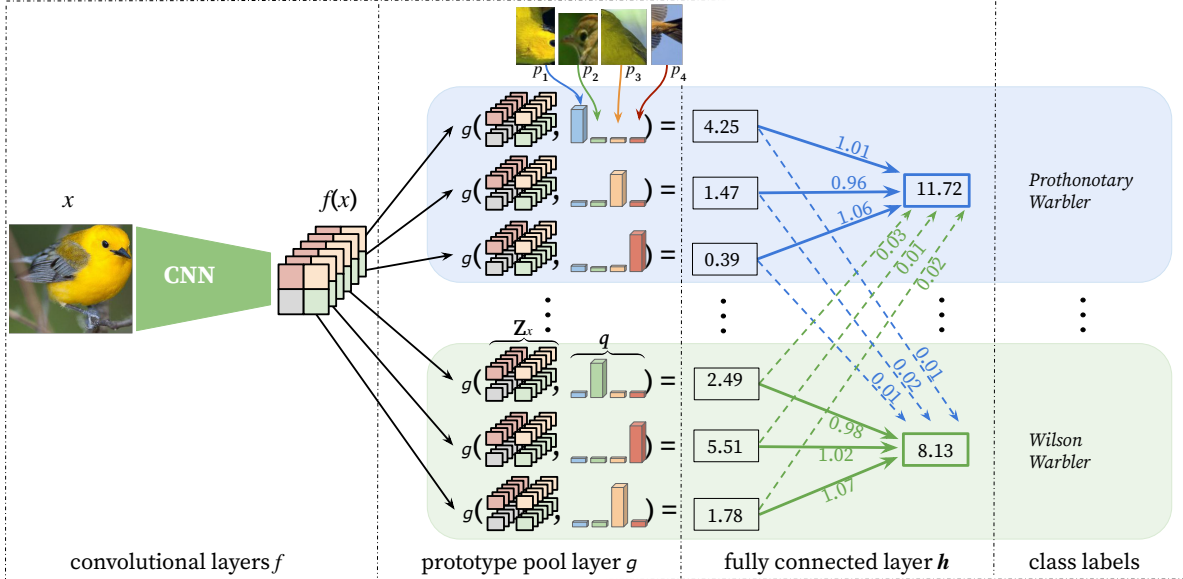


Figure 3. The architecture of our ProtoPool with a prototype pool layer g . Layer g contains a pool of prototypes $p_1 - p_4$ and 3 slots per class. Each slot is implemented as a distribution $q \in \mathbb{R}^4$ of prototypes available in the pool, where successive values of q correspond to the probability of assigning successive prototypes to the slot. In this example, p_1 and p_2 are assigned to the first slot of *Prothonotary Warbler* and *Wilson Warbler*, respectively. At the same time, the shared prototypes p_3 and p_4 are assigned to the second and third slots of both classes.

Prototypes Projection Prototypes projection is a step in the training process that allows prototypes visualization. More specifically, it replaces each abstract prototype learned by the model with the representation of the nearest training patch. For prototype p , it can be expressed by the following formula

$$p \leftarrow \arg \min_{z \in Z_C} \|z - p\|_2, \quad (3)$$

where $Z_C = \{z : z \in Z_x \text{ for all } (x, y) : y \in C\}$. In contrast to [8], set C is not a single class but the set of classes assigned to prototype p .

Theoretical Analysis Here, we theoretically analyze why the mechanisms introduced in the previous paragraphs force ProtoPool to assign one prototype per slot and assigned to different prototypes for class slots. For this purpose, we provide two observations.

OBSERVATION 1. Let $q \in [0, 1]^M$, $\sum q_i = 1$ be a distribution (slot) of a particular class. Then, the limit of Gumbel-softmax(q, τ), as τ approaches zero, is one of the canonical vector $e_i \in \mathbb{R}^M$, i.e. for q there exists $i = 1, \dots, M$ such that $\lim_{\tau \rightarrow 0} \text{Gumbel-softmax}(q, \tau) = e_i$.

The temperature parameter $\tau > 0$ controls how closely the new samples approximate discrete one-hot vectors (the canonical vector). From paper [23] we know that as $\tau \rightarrow 0$, the softmax computation smoothly approaches the arg max, and the sample vectors approach one-hot q distribution (see Figure 4).

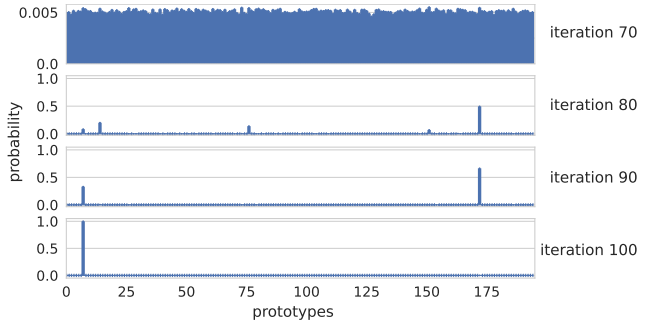


Figure 4. A sample distribution (slot) in the successive training steps (after 70, 80, 90, and 100 iterations). Till 70 iterations, all prototypes are assigned with a probability of 0.005. Then, the distribution binarizes, and after 100 iterations, one prototype is assigned to this slot with a probability close to one.

OBSERVATION 2. Let $K \in \mathbb{N}$ and q_1, \dots, q_K be the distributions (slots) of a particular class. If \mathcal{L}_{orth} defined in Eq. (1) is zero, then each prototype from a pool is assigned to only one slot of the class.

It follows the fact that $\mathcal{L}_{orth} = 0$ only if $\langle q_i, q_j \rangle = 0$ for all $i < j \leq K$, i.e. only if q_i, q_j have non-zero values for different prototypes.

4. Experiments

We train our model on CUB-200-2011 [56] and Stanford Cars [30] datasets to classify 200 bird species and

196 car models, respectively. As the convolutional layers f of the model, we take ResNet-34, ResNet-50, ResNet-121 [20], DenseNet-121, and DenseNet-161 [22] without the last layer, pretrained on ImageNet [11]. The one exception is ResNet-50 used with CUB-200-2011 datasets, which we pretrain on iNaturalist2017 [55] for fair comparison with ProtoTree model [39]. In the testing scenario, we make the prototype assignment hard meaning assigning 1.0 to the highest probability value. We set the number of prototypes assigned to each class to be at most 10 and use 202 and 195 prototypical parts for CUB-200-2011 and Stanford Cars, respectively. Details on experimental setup and results for other backbone networks are provided in the Supplementary Materials.

Comparison with other prototypical models In Table 1 we compare the efficiency of our ProtoPool with other models based on prototypical parts. We report the mean accuracy and standard error of the mean for 5 repetitions. Additionally, we present the number of prototypes used by the models, and we use this parameter to sort the results. We compare ProtoPool with ProtoPNet [8], ProtoPShare [48], ProtoTree [39], and TesNet [57].

One can observe that ProtoPool achieves the highest accuracy for the CUB-200-2011 dataset, surpassing even the models with a much larger number of prototypical parts (TesNet and ProtoPNet). For Stanford Cars, our model still performs better than other models with a similarly low number of prototypes, like ProtoTree and ProtoPShare, and slightly worse than TesNet, which uses ten times more prototypes. Overall, our method achieves competitive results with significantly fewer prototypes. It is important due to the theory of human cache memory [10].

5. Interpretability

In this section, we analyze the interpretability of the ProtoPool model. Firstly, we show that our model can be used both as a local and global explanation. Then, we discuss the differences between ProtoPool and other prototype-based approaches. We investigate if two classes share a similar number of prototypes in each run of the ProtoPool training. Then, we perform a user study on the similarity functions used by the ProtoPNet, ProtoTree, and ProtoPool to assess their understandability by the humans. Lastly, we consider ProtoPool from the cognitive psychology perspective.

Local and global interpretations In Figure 1, we show how two classes share prototypical parts. One can observe that between any two classes (in this case *Prothonotary Warbler* and *Wilson Warbler*), we can present three sets of prototypical parts: specific for the first class, for the second class, and common for both of them. That way, ProtoPool can globally describe the relations between classes relying only on the positive reasoning process. In contrast, Pro-

Data	Model	Architecture	Proto. #	Acc [%]
CUB-200-2011	ProtoPool (ours)	ResNet34	202	80.3 ± 0.2
	ProtoPShare [48]		400	74.7
	ProtoPNet [8]		1655	79.5
	TesNet [57]		2000	82.7 ± 0.2
	ProtoPool (ours)	ResNet152	202	81.5 ± 0.1
	ProtoPShare [48]		1000	73.6
	ProtoPNet [8]		1734	78.6
	TesNet [57]		2000	82.8 ± 0.2
	ProtoPool (ours)	iNat ResNet50	202	85.5 ± 0.1
	ProtoTree [39]		202	82.2 ± 0.7
	ProtoPool (ours)	Ensemble x3	202 × 3	87.5
	ProtoTree [39]		202 × 3	86.6
	ProtoPool (ours)	Ensemble x5	202 × 5	87.6
	ProtoTree [39]		202 × 5	87.2
	ProtoPNet [8]		2000 × 5	84.8
	TesNet [57]		2000 × 5	86.2
Stanford Cars	ProtoPool (ours)	ResNet34	195	89.3 ± 0.1
	ProtoPShare [48]		480	86.4
	ProtoPNet [8]		1960	86.1 ± 0.2
	TesNet [57]		1960	92.6 ± 0.3
	ProtoPool (ours)	ResNet50	195	88.9 ± 0.1
	ProtoTree [39]		195	86.6 ± 0.2
	ProtoPool (ours)	Ensemble x3	195 × 3	91.1
	ProtoTree [39]		195 × 3	90.5
	ProtoPool (ours)	Ensemble x5	195 × 5	91.6
	ProtoTree [39]		195 × 5	91.5
	ProtoPNet [8]		1960 × 5	91.4
	TesNet [57]		1960 × 5	93.1

Table 1. Comparison of ProtoPool with other methods based on prototypical parts trained on the CUB-200-2011 and Stanford Cars datasets, considering a various number of prototypes and types of convolutional layers f . One can observe that ProtoPool achieves the best results both for an individual model and ensemble predictions, even for models with ten times more prototypes in the case of CUB-200-2011 dataset. Also, ensemble of 3 ProtoPools surpasses ensemble of 5 TesNets with 17 times more prototypes. On the other hand, in the case of Stanford Cars ProtoPool achieves competitive results with significantly fewer prototypes. Please note that the results are first sorted by backbone network and then by the number of prototypes.

toTree also uses negative reasoning, as it identifies a class by lacking features. This hinders meaningful global explanations because a user would have to analyze all prototypical parts, considering that they do not describe the class. A global data class characterization is presented in Figure 5, where we show the prototypical parts of *Scarlet Tanager*. One can observe that found prototypes correspond to the visual features of this species, such as red feathers, puffy belly, and short beak. Similar to ProtoPShare, ProtoPool shares the prototypical parts between data classes. It allows

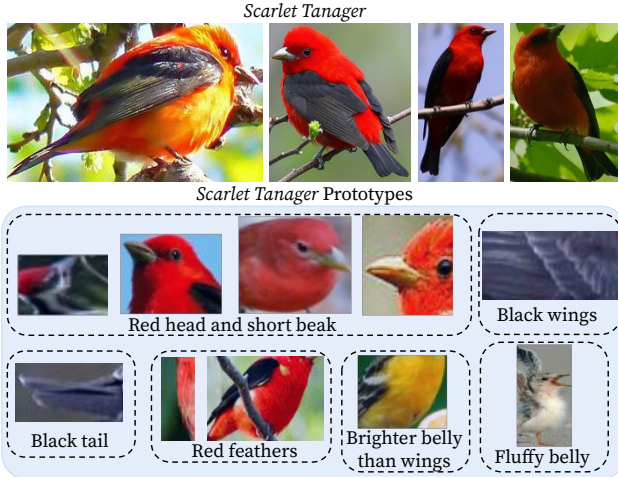


Figure 5. Samples of *Scarlet Tanager* with prototypical parts associated with this class by our ProtoPool model. Among others, one can observe prototypes corresponding to red feathers, fluffy belly, black wings and tail, and belly brighter than the wings³.

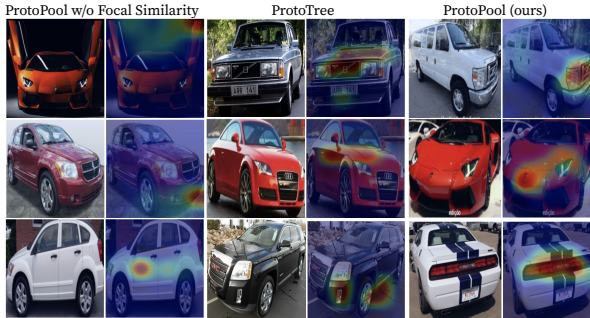


Figure 6. Examples of prototype activation maps obtained with models using various similarity functions. One can observe that ProtoPool with the focal similarity is the only one that focuses on car features like a spoiler, reflector, and *Ferrari* logo when the other similarities focus on image borders or much larger regions.

to discover similarities between data classes and present them to the user (see example in Supplementary Materials). In addition, we visualize the prototypical part shared between 9 data classes in Figure 9. The local explanations of ProtoPool are similar to those from ProtoPNet, TesNet, and ProtoPShare. An example is presented in Figure 7.

Interpretability features comparison In Table 2, we compare the characteristics of various prototypical-based methods. Firstly, ProtoPool and ProtoTree utilize fewer prototypical parts than the ProtoPNet and TesNet (around 10%). ProtoPShare also uses fewer prototypes (up to 20%), but it requires a trained ProtoPNet model before performing merge-pruning. Regarding class similarity, it is directly obtained from ProtoPool slots, in contrast to ProtoTree, which requires traversing through the decision tree. Naturally,

³Names of prototypical parts are provided by the authors.

Model	Portion of prototypes	Reasoning type	Prototype sharing
ProtoPool	~10%	+	direct
ProtoTree	~10%	+ -	indirect
ProtoPShare	[20%;50%]	+	direct
ProtoPNet	100%	+	none
TesNet	100%	+	none

Table 2. Characteristics of prototype-based methods for fine-grained image classification that considers the number of prototypes, reasoning type, and prototype sharing between classes. One can observe that ProtoPool uses 10% of ProtoPNet’s prototypes using only positive reasoning. It shares the prototypes between classes, but in contrast to ProtoPShare, it is trained in an end-to-end, fully differentiable manner. Please notice that 100% corresponds to 2000 and 1960 for CUB-200-2011 and Stanford Cars datasets, respectively.

Why is that *Ford Freestar Minivan 2007*?

Image	Prototypical part	Activation map	Similarity and weight
			$4.08 \cdot 0.89 = 3.63$
			$3.87 \cdot 0.83 = 3.21$
	⋮	⋮	⋮
			$3.82 \cdot 0.81 = 3.09$
			SUM: 21.64

Figure 7. Example explanation of predicting *Ford Freestar Minivan 2007*. Except for an image, we present a few prototypical parts of this class, their activation maps, similarity function values, and the last layer’s weights. As an output, we return a class with the highest sum of the similarities multiplied by the weights.

ProtoPNet and TesNet have no mechanism to detect inter-class similarities. Finally, ProtoTree depends on *negative* reasoning process, while in the case of ProtoPool, it relies only on the positive reasoning process, which is a desirable feature according to [8].

Stability of shared prototypes The natural question that appears when analyzing the assignment of the prototypes is: *Does the similarity between two classes hold for many runs of ProtoPool training?* To analyze this behavior, in Figure 8 we show how the distribution of the number of classes sharing a prototype differs between runs. One can observe that difference between runs is negligible. In all runs, most prototypes are shared by five classes, but there exist prototypes shared by more than thirty classes. On average, a prototype is shared by 2.73 ± 0.51 . An example inter-class similarity graph is presented in the Supplementary Materials.

User study on focal similarity perception To validate if using focal similarity results in more significant prototyp-

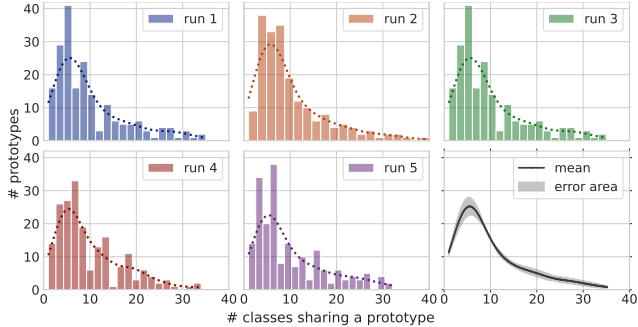


Figure 8. Distribution of the number of classes sharing a prototype presented as a histogram with an estimation plot (dashed line). Each color corresponds to a single ProtoPool training on Stanford Cars dataset with ResNet50 a backbone network. The bottom right plot corresponds to the mean and standard deviation for five runs. One can observe that the distribution is similar between runs, showing model stability.

ical parts, we performed a user study where we asked the participant to answer the question: “*Is the feature pointed by the model distinctive for the class of a given object?*” We used 60 random images (30 for each dataset) presented in random order and gave unlimited time for an answer. Each question consisted of an original training image and the same image with overlaid activation map, as in Figure 6. The task was to assign a score from 1 to 5 where 1 meant “*I am certain that this is NOT a distinctive feature*” and 5 meant “*I am sure that this feature is distinctive*”. Images are generated using prototypes obtained for ProtoPool with ProtoPNets similarity or with focal similarity and from a trained ProtoTree⁴.

Results presented in Figure 10 show that ProtoPool obtains mostly scores 4 and 5, while other methods often obtain score 1. Hence, we conclude that ProtoPool with focal similarity generated more meaningful prototypes than the reference models, including ProtoTree. See Supplementary Materials for detailed results and a sample questionnaire.

ProtoPool in the context of cognitive psychology When comparing different prototypical models in the light of cognitive science, we consider the number of prototypes (due to the theory of human cache memory [10]) and reasoning type. ProtoPool has significantly fewer prototypes than ProtoPNet, TesNet, and ProtoPShare. Moreover, it has a different reasoning type and information representation than ProtoTree. ProtoPool can be described in terms of parallel or simultaneous information processing, while ProtoTree may be characterized by serial or successive processing, which takes more time [25, 34, 40]. More specifically, human cognition is marked with the speed-accuracy trade-off. De-

⁴ProtoTree was trained using code from <https://github.com/M-Nauta/ProtoTree> and obtained accuracy similar to [39]. For ProtoPNet similarity, we used code from <https://github.com/cfchen-duke/ProtoPNet>.

Architecture	Dataset	Acc [%] before	Acc [%] after
ResNet34	Birds	80.8 ± 0.2	80.3 ± 0.2
ResNet152		81.2 ± 0.2	81.5 ± 0.1
iNat ResNet50		85.9 ± 0.1	85.5 ± 0.1
ResNet34	Cars	89.1 ± 0.2	89.3 ± 0.1
ResNet50		88.4 ± 0.1	88.9 ± 0.1

Table 3. The influence of prototype projection on ProtoPool performance for CUB-200-2011 (Birds) and Stanford Cars (Cars) datasets. Note that the accuracy after projection is preserved.

pending on the perceptual situation and the goal of a task, the human mind can apply a categorization process (simultaneous or successive) that is the most appropriate in a given context, i.e. the fastest or the most accurate. Both models have their advantages. However, ProtoTree has a specific shortcoming because it allows for a categorization process to rely on an absence of features. In other words, an object characterized by none of the enlisted features is labeled as a member of a specific category. This type of reasoning is useful when the amount of information to be processed (i.e. number of features and categories) is fixed and relatively small. However, the time of object categorization profoundly elongates if the number of categories (and therefore the number of features to be crossed out) is high. Also, the chance of miscategorizing completely new information is increased. Therefore, the general rule of opting for quick and adequate solutions known as cognitive miser [12] seems to be met in our ProtoPool.

6. Ablation study

In this section, we analyze how the prototype projection, the novel architectural choices, and the number of prototypes influence the overall model performance.

Before and after prototype projection Since ProtoPool has much fewer prototypical parts than other models based on a positive reasoning process, applying projection could result in insignificant prototypes. Hence, in Table 3 we investigate the influence of the prototypes projection on ProtoPool, showing that it preserves its effectiveness.

Influence of the novel architectural choices Additionally, we analyze the influence of the novel components we introduce on the final results. For this purpose, we train ProtoPool with softmax instead of Gumbel-Softmax trick, without orthogonalization loss, and with similarity from ProtoPNet instead of focal similarity. Results are presented in Table 4 and in Supplementary Materials. We observe that Gumbel-Softmax trick has a significant influence on the model performance, especially for the Stanford Cars dataset, probably due to lower inter-class similarity than in CUB-200-2011 dataset [39]. On the other hand, the focal similarity does not influence model accuracy, although as



Figure 9. Sample prototype shared by nine classes, which describes a *convex tailgate*. Please notice that most of the cars are luxury, but some exceptions also contain a *convex tailgate* (e.g. *Fiat 500*).

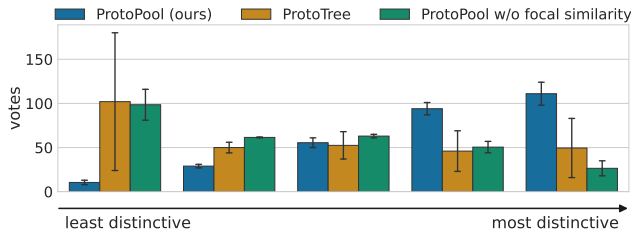


Figure 10. Distribution of scores from user study on prototypes obtained for ProtoPool without and with focal similarity and for ProtoTree. One can observe that ProtoPool with focal similarity generated more meaningful prototypes than the reference models.

Model	Dataset	Acc [%]
ProtoPool		85.5
w/o \mathcal{L}_{orth}		82.4
w/o Gumbel-Softmax trick	Birds	80.3
w/o Gumbel-Softmax trick and \mathcal{L}_{orth}		65.1
w/o focal similarity		85.3
ProtoPool		88.9
w/o \mathcal{L}_{orth}		86.8
w/o Gumbel-Softmax trick	Cars	64.5
w/o Gumbel-Softmax trick and \mathcal{L}_{orth}		30.8
w/o focal similarity		88.8

Table 4. Influence of novel architectural choices on ProtoPool performance for CUB-200-2011 (Birds) and Stanford Cars (Cars) datasets. We consider training with softmax instead of Gumbel-Softmax, without orthogonalization loss, and with similarity from ProtoPNet instead of focal similarity. One can observe that the mix of the proposed mechanisms obtains the best results.

presented in Section 5, it has a positive impact on the interpretability. When it comes to orthogonality, it slightly increases the model accuracy thanks to forcing diversity in class slots. Finally, the mix of the proposed mechanisms obtains the best results.

Number of prototypes vs accuracy Finally, in Figure 11 we investigate how the number of prototypical parts influences accuracy for the CUB-200-2011 (blue) and Stanford Cars (red) datasets. We observe that up to around 200 prototypical parts, models’ accuracy increases and reaches the plateau. Therefore, we conclude that the amount of prototypes optimal for ProtoTree is also optimal for ProtoPool.

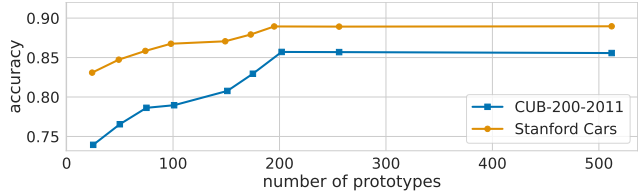


Figure 11. ProtoPool accuracy depending on the number of prototypical parts for CUB-200-2011 (blue square) and Stanford Cars (orange circle) datasets. One can observe that the model reaches a plateau for around 200 prototypical parts, and there is no gain in further increase of prototype number.

7. Conclusions

We presented ProtoPool, a self-explainable method that incorporates the paradigm of prototypical parts to explain its predictions. This model shares the prototypes between classes without pruning operations, reducing their number up to ten times. Moreover, it is fully differentiable. To efficiently assign the prototypes to classes, we apply Gumbel-Softmax trick together with orthogonalization loss. Additionally, we introduced focal similarity that focuses on rare foreground features. As a result, we increased the model’s interpretability while maintaining high accuracy, as we showed through theoretical analysis and many experiments, including user study.

Discussion of limitations Our ProtoPool model inherits its limitations from the other prototype-based models, including non-obvious prototype meaning. Hence, even after prototype projection from a training dataset, there is still uncertainty on which attributes it represents. However, there exist ways to mitigate this limitation, e.g. using a framework defined in [38]. Additionally, the choice of Gumbel-Softmax temperature τ and its decreasing strategy are not straightforward and require a careful hyperparameter search. Lastly, in the case of ProtoPool, increasing the number of prototypes does not increase the model accuracy after some point because the model saturates.

Discussion of negative impact We base our solution on prototypical parts, which are vulnerable to a new type of adversarial attacks [21]. Hence, practitioners must consider this danger when deploying a system with a ProtoPool. Additionally, it can spread disinformation when prototypes de-

rive from spoiled data or are presented without an expert comment, especially in fields like medicine.

Acknowledgments

This research was supported by: grant no POIR.04.04.00-00-14DE/18-00 carried out within the Team-Net program of the Foundation for Polish Science co-financed by the European Union under the European Regional Development Fund. This research was funded by the National Science Centre, Poland (research grant no. 2020/39/D/ST6/01332). For the purpose of Open Access, the authors have applied a CC-BY public copyright licence to any Author Accepted Manuscript (AAM) version arising from this submission.

References

- [1] Ehsan Abbasnejad, Damien Teney, Amin Parvaneh, Javen Shi, and Anton van den Hengel. Counterfactual vision and language learning. In *Proceedings of the IEEE/CVF Conference on Computer Vision and Pattern Recognition*, pages 10044–10054, 2020. 2
- [2] Julius Adebayo, Justin Gilmer, Michael Muelly, Ian Goodfellow, Moritz Hardt, and Been Kim. Sanity checks for saliency maps. In S. Bengio, H. Wallach, H. Larochelle, K. Grauman, N. Cesa-Bianchi, and R. Garnett, editors, *Advances in Neural Information Processing Systems*, volume 31. Curran Associates, Inc., 2018. 2
- [3] Michael Anis Mihdi Afnan, Yanhe Liu, Vincent Conitzer, Cynthia Rudin, Abhishek Mishra, Julian Savulescu, and Masoud Afnan. Interpretable, not black-box, artificial intelligence should be used for embryo selection. *Human Reproduction Open*, 2021. 1, 3
- [4] David Alvarez Melis and Tommi Jaakkola. Towards robust interpretability with self-explaining neural networks. In S. Bengio, H. Wallach, H. Larochelle, K. Grauman, N. Cesa-Bianchi, and R. Garnett, editors, *Advances in Neural Information Processing Systems*, volume 31. Curran Associates, Inc., 2018. 1, 2
- [5] Alina Jade Barnett, Fides Regina Schwartz, Chaofan Tao, Chaofan Chen, Yin hao Ren, Joseph Y Lo, and Cynthia Rudin. Iaia-bl: A case-based interpretable deep learning model for classification of mass lesions in digital mammography. *arXiv preprint arXiv:2103.12308*, 2021. 3
- [6] Dominika Basaj, Witold Oleszkiewicz, Igor Sieradzki, Michał Górszczak, B Rychalska, T Trzcinski, and B Zielinski. Explaining self-supervised image representations with visual probing. In *International Joint Conference on Artificial Intelligence*, 2021. 1, 2
- [7] Wieland Brendel and Matthias Bethge. Approximating CNNs with bag-of-local-features models works surprisingly well on imagenet. In *International Conference on Learning Representations*, 2019. 1, 2
- [8] Chaofan Chen, Oscar Li, Daniel Tao, Alina Barnett, Cynthia Rudin, and Jonathan K Su. This looks like that: deep learning for interpretable image recognition. In *NeurIPS*, pages 8930–8941, 2019. 1, 2, 3, 4, 5, 6, 12, 13
- [9] Zhi Chen, Yijie Bei, and Cynthia Rudin. Concept whitening for interpretable image recognition. *Nature Machine Intelligence*, 2(12):772–782, 2020. 2
- [10] Nelson Cowan. Working memory capacity limits in a theoretical context. In *Human learning and memory: Advances in theory and application. The 4th Tsukuba international conference on memory*, pages 155–175. Erlbaum, 2005. 5, 7
- [11] Jia Deng, Wei Dong, Richard Socher, Li-Jia Li, Kai Li, and Li Fei-Fei. Imagenet: A large-scale hierarchical image database. In *2009 IEEE conference on computer vision and pattern recognition*, pages 248–255. Ieee, 2009. 5
- [12] Susan T Fiske and Shelley E Taylor. *Social cognition*. McGraw-Hill Book Company, 1991. 7, 12, 14
- [13] Ruth Fong, Mandela Patrick, and Andrea Vedaldi. Understanding deep networks via extremal perturbations and smooth masks. In *Proceedings of the IEEE/CVF International Conference on Computer Vision*, pages 2950–2958, 2019. 2
- [14] Ruth C Fong and Andrea Vedaldi. Interpretable explanations of black boxes by meaningful perturbation. In *Proceedings of the IEEE international conference on computer vision*, pages 3429–3437, 2017. 2
- [15] Alan H Gee, Diego Garcia-Olano, Joydeep Ghosh, and David Paydarfar. Explaining deep classification of time-series data with learned prototypes. In *CEUR workshop proceedings*, volume 2429, page 15. NIH Public Access, 2019. 3
- [16] Amirata Ghorbani, James Wexler, James Y Zou, and Been Kim. Towards automatic concept-based explanations. In H. Wallach, H. Larochelle, A. Beygelzimer, F. d'Alché-Buc, E. Fox, and R. Garnett, editors, *Advances in Neural Information Processing Systems*, volume 32. Curran Associates, Inc., 2019. 2
- [17] Yash Goyal, Ziyan Wu, Jan Ernst, Dhruv Batra, Devi Parikh, and Stefan Lee. Counterfactual visual explanations. In *International Conference on Machine Learning*, pages 2376–2384. PMLR, 2019. 2
- [18] Riccardo Guidotti, Anna Monreale, Stan Matwin, and Dino Pedreschi. Explaining image classifiers generating exemplars and counter-exemplars from latent representations. *Proceedings of the AAAI Conference on Artificial Intelligence*, 34(09):13665–13668, Apr. 2020. 2
- [19] Peter Hase, Chaofan Chen, Oscar Li, and Cynthia Rudin. Interpretable image recognition with hierarchical prototypes. In *Proceedings of the AAAI Conference on Human Computation and Crowdsourcing*, volume 7, pages 32–40, 2019. 3
- [20] Kaiming He, Xiangyu Zhang, Shaoqing Ren, and Jian Sun. Deep residual learning for image recognition. In *Proceedings of the IEEE conference on computer vision and pattern recognition*, pages 770–778, 2016. 5
- [21] Adrian Hoffmann, Claudio Fanconi, Rahul Rade, and Jonas Kohler. This looks like that... does it? shortcomings of latent space prototype interpretability in deep networks. *arXiv preprint arXiv:2105.02968*, 2021. 8
- [22] Gao Huang, Zhuang Liu, Laurens Van Der Maaten, and Kilian Q Weinberger. Densely connected convolutional networks. In *Proceedings of the IEEE conference on computer vision and pattern recognition*, pages 4700–4708, 2017. 5

- [23] Eric Jang, Shixiang Gu, and Ben Poole. Categorical reparameterization with gumbel-softmax. *arXiv:1611.01144*, 2016. 3, 4
- [24] Margot E Kaminski. The right to explanation, explained. In *Research Handbook on Information Law and Governance*. Edward Elgar Publishing, 2021. 1
- [25] Raymond Kesner. A neural system analysis of memory storage and retrieval. *Psychological Bulletin*, 80(3):177, 1973. 7
- [26] Been Kim, Martin Wattenberg, Justin Gilmer, Carrie Cai, James Wexler, Fernanda Viegas, et al. Interpretability beyond feature attribution: Quantitative testing with concept activation vectors (tcav). In *International conference on machine learning*, pages 2668–2677. PMLR, 2018. 1, 2
- [27] Eunji Kim, Siwon Kim, Minji Seo, and Sungroh Yoon. Xprotonet: Diagnosis in chest radiography with global and local explanations. In *Proceedings of the IEEE/CVF Conference on Computer Vision and Pattern Recognition*, pages 15719–15728, 2021. 3
- [28] Diederik P. Kingma and Jimmy Lei Ba. Adam: A method for stochastic optimization. In *ICLR 2015 : International Conference on Learning Representations 2015*, 2015. 12
- [29] Pang Wei Koh, Thao Nguyen, Yew Siang Tang, Stephen Mussmann, Emma Pierson, Been Kim, and Percy Liang. Concept bottleneck models. In Hal Daumé III and Aarti Singh, editors, *Proceedings of the 37th International Conference on Machine Learning*, volume 119 of *Proceedings of Machine Learning Research*, pages 5338–5348. PMLR, 13–18 Jul 2020. 2
- [30] Jonathan Krause, Michael Stark, Jia Deng, and Li Fei-Fei. 3d object representations for fine-grained categorization. In *Proceedings of the IEEE international conference on computer vision workshops*, pages 554–561, 2013. 4, 12
- [31] Oscar Li, Hao Liu, Chaofan Chen, and Cynthia Rudin. Deep learning for case-based reasoning through prototypes: A neural network that explains its predictions. In *Proceedings of the AAAI Conference on Artificial Intelligence*, volume 32, 2018. 1, 3
- [32] Nian Liu, Ni Zhang, Kaiyuan Wan, Ling Shao, and Junwei Han. Visual saliency transformer. In *Proceedings of the IEEE/CVF International Conference on Computer Vision*, pages 4722–4732, 2021. 2
- [33] Scott M Lundberg and Su-In Lee. A unified approach to interpreting model predictions. In *Proceedings of the 31st international conference on neural information processing systems*, pages 4768–4777, 2017. 1
- [34] AR Luria. The origin and cerebral organization of man’s conscious action. *Children with learning problems: Readings in a developmental-interaction*. New York, Brunner/Mazel, pages 109–130, 1973. 7
- [35] Diego Marcos, Sylvain Lobry, and Devis Tuia. Semantically interpretable activation maps: what-where-how explanations within cnns. In *2019 IEEE/CVF International Conference on Computer Vision Workshop (ICCVW)*, pages 4207–4215. IEEE, 2019. 2
- [36] Yao Ming, Panpan Xu, Huamin Qu, and Liu Ren. Interpretable and steerable sequence learning via prototypes. In *Proceedings of the 25th ACM SIGKDD International Conference on Knowledge Discovery & Data Mining*, pages 903–913, 2019. 3
- [37] Ramaravind K Mothilal, Amit Sharma, and Chenhao Tan. Explaining machine learning classifiers through diverse counterfactual explanations. In *Proceedings of the 2020 Conference on Fairness, Accountability, and Transparency*, pages 607–617, 2020. 2
- [38] Meike Nauta, Annemarie Jutte, Jesper Provoost, and Christin Seifert. This looks like that, because... explaining prototypes for interpretable image recognition. *arXiv preprint arXiv:2011.02863*, 2020. 8, 12
- [39] Meike Nauta, Ron van Bree, and Christin Seifert. Neural prototype trees for interpretable fine-grained image recognition. In *Proceedings of the IEEE/CVF Conference on Computer Vision and Pattern Recognition*, pages 14933–14943, 2021. 1, 2, 3, 5, 7, 13
- [40] Ubric Neisser. *Cognitive psychology* (new york: Appleton). Century, Crofts, 1967. 7
- [41] Yulei Niu, Kaihua Tang, Hanwang Zhang, Zhiwu Lu, Xian-Sheng Hua, and Ji-Rong Wen. Counterfactual vqa: A cause-effect look at language bias. In *Proceedings of the IEEE/CVF Conference on Computer Vision and Pattern Recognition*, pages 12700–12710, 2021. 2
- [42] Esther Puyol-Antón, Chen Chen, James R Clough, Bram Ruijsink, Baldeep S Sidhu, Justin Gould, Bradley Porter, Marc Elliott, Vishal Mehta, Daniel Rueckert, et al. Interpretable deep models for cardiac resynchronisation therapy response prediction. In *International Conference on Medical Image Computing and Computer-Assisted Intervention*, pages 284–293. Springer, 2020. 2
- [43] Sylvestre-Alvise Rebuffi, Ruth Fong, Xu Ji, and Andrea Vedaldi. There and back again: Revisiting backpropagation saliency methods. In *Proceedings of the IEEE/CVF Conference on Computer Vision and Pattern Recognition*, pages 8839–8848, 2020. 2
- [44] Marco Tulio Ribeiro, Sameer Singh, and Carlos Guestrin. ” why should i trust you?” explaining the predictions of any classifier. In *Proceedings of the 22nd ACM SIGKDD international conference on knowledge discovery and data mining*, pages 1135–1144, 2016. 1, 2
- [45] Eleanor Rosch. Cognitive representations of semantic categories. *Journal of experimental psychology: General*, 104(3):192, 1975. 1
- [46] Eleanor H Rosch. Natural categories. *Cognitive psychology*, 4(3):328–350, 1973. 1
- [47] Cynthia Rudin. Stop explaining black box machine learning models for high stakes decisions and use interpretable models instead. *Nature Machine Intelligence*, 1(5):206–215, 2019. 2
- [48] Dawid Rymarczyk, Łukasz Struski, Jacek Tabor, and Bartosz Zieliński. Protoshare: Prototypical parts sharing for similarity discovery in interpretable image classification. In *Proceedings of the 27th ACM SIGKDD Conference on Knowledge Discovery & Data Mining*, pages 1420–1430, 2021. 1, 2, 3, 5, 13
- [49] Ramprasaath R Selvaraju, Michael Cogswell, Abhishek Das, Ramakrishna Vedantam, Devi Parikh, and Dhruv Batra.

- Grad-cam: Visual explanations from deep networks via gradient-based localization. In *Proceedings of the IEEE international conference on computer vision*, pages 618–626, 2017. [1](#), [2](#)
- [50] Ramprasaath R Selvaraju, Stefan Lee, Yilin Shen, Hongxia Jin, Shalini Ghosh, Larry Heck, Dhruv Batra, and Devi Parikh. Taking a hint: Leveraging explanations to make vision and language models more grounded. In *Proceedings of the IEEE/CVF International Conference on Computer Vision*, pages 2591–2600, 2019. [2](#)
- [51] Karen Simonyan, Andrea Vedaldi, and Andrew Zisserman. Deep inside convolutional networks: Visualising image classification models and saliency maps. In *In Workshop at International Conference on Learning Representations*. Citeseer, 2014. [2](#)
- [52] Gurmail Singh and Kin-Choong Yow. These do not look like those: An interpretable deep learning model for image recognition. *IEEE Access*, 9:41482–41493, 2021. [3](#)
- [53] Mukund Sundararajan, Ankur Taly, and Qiqi Yan. Axiomatic attribution for deep networks. In *International Conference on Machine Learning*, pages 3319–3328. PMLR, 2017. [2](#)
- [54] Sunil Thulasidasan, Gopinath Chennupati, Jeff A. Bilmes, Tanmoy Bhattacharya, and Sarah Michalak. On mixup training: Improved calibration and predictive uncertainty for deep neural networks. In *Advances in Neural Information Processing Systems*, volume 32, pages 13888–13899, 2019. [12](#)
- [55] Grant Van Horn, Oisin Mac Aodha, Yang Song, Yin Cui, Chen Sun, Alex Shepard, Hartwig Adam, Pietro Perona, and Serge Belongie. The inaturalist species classification and detection dataset. In *Proceedings of the IEEE conference on computer vision and pattern recognition*, pages 8769–8778, 2018. [5](#)
- [56] Catherine Wah, Steve Branson, Peter Welinder, Pietro Perona, and Serge Belongie. The caltech-ucsd birds-200-2011 dataset. 2011. [4](#), [12](#)
- [57] Jiaqi Wang, Huafeng Liu, Xinyue Wang, and Liping Jing. Interpretable image recognition by constructing transparent embedding space. In *Proceedings of the IEEE/CVF International Conference on Computer Vision*, pages 895–904, 2021. [2](#), [3](#), [5](#), [13](#)
- [58] Pei Wang and Nuno Vasconcelos. Scout: Self-aware discriminant counterfactual explanations. In *Proceedings of the IEEE/CVF Conference on Computer Vision and Pattern Recognition*, pages 8981–8990, 2020. [2](#)
- [59] Gesa Wiegand, Matthias Schmidmaier, Thomas Weber, Yuanting Liu, and Heinrich Hussmann. I drive-you trust: Explaining driving behavior of autonomous cars. In *Extended abstracts of the 2019 chi conference on human factors in computing systems*, pages 1–6, 2019. [1](#)
- [60] Tianjun Xiao, Yichong Xu, Kuiyuan Yang, Jiaying Zhang, Yuxin Peng, and Zheng Zhang. The application of two-level attention models in deep convolutional neural network for fine-grained image classification. In *Proceedings of the IEEE conference on computer vision and pattern recognition*, pages 842–850, 2015. [2](#)
- [61] Chih-Kuan Yeh, Been Kim, Sercan Arik, Chun-Liang Li, Tomas Pfister, and Pradeep Ravikumar. On completeness-aware concept-based explanations in deep neural networks. In H. Larochelle, M. Ranzato, R. Hadsell, M. F. Balcan, and H. Lin, editors, *Advances in Neural Information Processing Systems*, volume 33, pages 20554–20565. Curran Associates, Inc., 2020. [2](#)
- [62] Heliang Zheng, Jianlong Fu, Tao Mei, and Jiebo Luo. Learning multi-attention convolutional neural network for fine-grained image recognition. In *Proceedings of the IEEE international conference on computer vision*, pages 5209–5217, 2017. [2](#)
- [63] Heliang Zheng, Jianlong Fu, Zheng-Jun Zha, and Jiebo Luo. Looking for the devil in the details: Learning trilinear attention sampling network for fine-grained image recognition. In *Proceedings of the IEEE/CVF Conference on Computer Vision and Pattern Recognition*, pages 5012–5021, 2019. [1](#), [2](#)
- [64] Bolei Zhou, Yiyou Sun, David Bau, and Antonio Torralba. Interpretable basis decomposition for visual explanation. In *Proceedings of the European Conference on Computer Vision (ECCV)*, pages 119–134, 2018. [2](#)

Supplementary materials

Experimental setup

Here, we present the details of the experimental setup. We use two datasets: CUB-200-2011 [56] consisted of 200 species of birds and Stanford Cars [30] with 196 car models. For both datasets, images are augmented offline using parameters from Table 5, and the process of data preparation is the same as in [8]⁵.

Our model consists of the convolutional part f that is a convolutional block from ResNet or DenseNet followed by 1×1 convolutional layer to transform the latent space depth to be 128 for Stanford Cars and 256 for CUB-200-2011. We perform a warmup training where the weights of f are frozen for 10 epochs, and then we train the model until it converges with 12 epochs early stopping. After convergence, we perform prototype projection and fine-tune the last layer. We use the learning schema presented in Table 6.

Additionally, we use Adam optimizer [28] with parameters $\beta_1 = 0.9$ and $\beta_2 = 0.999$. We set the batch size equal 80 and use images of input size $224 \times 224 \times 3$. We use prototypical parts of size $1 \times 1 \times \{128, 256\}$ for Stanford Cars and CUB-200-2011 respectively. When the model is initialized, the last layer weights are 1 for the connection between the class logit and its slots, all other are set to be 0. All other parameters are initialized with Xavier normal initializer.

We use the Gumbel-Softmax trick to assign prototypes to slots of a class unambiguously. However, in contrast to the classic variant of this parametrization trick, we reduce the influence of the noise in subsequent iterations. For this purpose, we use $y^i = \frac{\exp(q^i/\tau + \eta_i)}{\sum_{m=1}^M \exp(q^m/\tau + \eta_m)}$ instead of $y^i = \frac{\exp((q^i + \eta_i)/\tau)}{\sum_{m=1}^M \exp((q^m + \eta_m)/\tau)}$ in Gumbel-Softmax distribution

$$\text{Gumbel-softmax}(q, \tau) = (y^1, \dots, y^M) \in \mathbb{R}^M,$$

where $\tau \in (0, \infty)$ and $q \in \mathbb{R}^M$. Moreover, we start the Gumbel-Softmax distribution with $\tau = 1$ and we decrease it till 0.001 for 30 epochs. As a decrease function we use:

$$\tau(\text{epoch}) = \begin{cases} 1/\sqrt{\alpha \cdot \text{epoch}} & \text{if epoch} < 30 \\ 0.001 & \text{otherwise} \end{cases},$$

where $\alpha = 3.4 \cdot 10^4$. We use the following weighting schema for loss function: $\mathcal{L}_{entropy} = 1.0$, $\mathcal{L}_{clst} = 0.8$, $\mathcal{L}_{sep} = -0.08$, $\mathcal{L}_{orth} = 1.0$, and $\mathcal{L}_{l_1} = 10^{-4}$. Moreover, we normalize \mathcal{L}_{orth} , dividing it by the number of classes multiplied by the number of slots per class.

Additional results

In Table 7, we present the results for DenseNet as a backbone of our ProtoPool model.

⁵see Instructions for preparing the data at <https://github.com/cfchen-duke/ProtoPNet>

Augmentation	Value	Probability
Rotation	$[-15^\circ, 15^\circ]$	1.0
Flip	Vertical	0.5
Flip	Horizontal	0.5
Skew	$< 45^\circ$	0.5
Shear	$[-10^\circ, 10^\circ]$	1.0
Mix-up [54]	50% : 50%	1.0

Table 5. Augmentation policy.

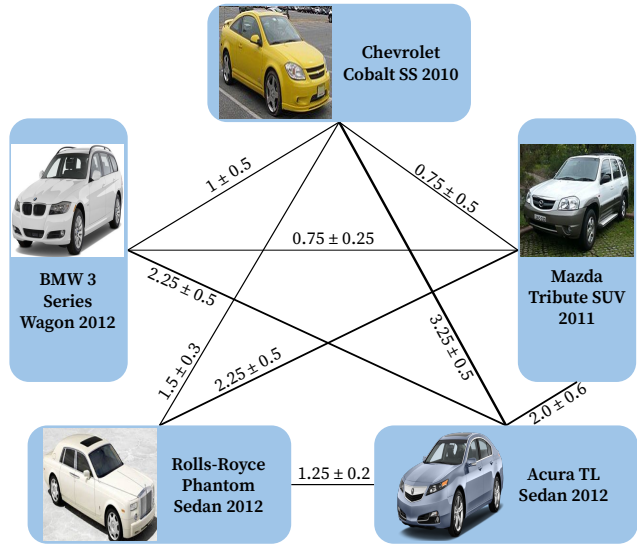


Figure 12. We present a Sample graph obtained from ProtoPool for five classes from the Stanford Cars dataset. Each class is represented by a single image, and the edges correspond to the mean number of prototypes shared between classes over five repetitions. One can observe that ProtoPool discovered similarities between SUVs and Sedans, while Rolls-Royce and BMW have nothing in common. Moreover, the graphs are consistent between runs and discover similar relations between classes.

Detailed comparison of the prototypical models

In Table 8, we present the extended version of prototypical-based model comparison. One can observe that ProtoPool is the only one that has a differentiable prototypical parts assignment. Additionally, it processes the data simultaneously, which is faster and easier to comprehend by humans [12] than sequential processing obtained from the ProtoTree [38]. Lastly, ProtoPool, as ProtoPShare, directly provides class similarity that is visualized in the Figure 12.

Additional ablation study

Referring to Table 4 of the paper, where we present the influence of novel architectural choices on ProtoPool performance, we provide corresponding matrices of prototype assignment in Figures 13 and 15 for CUB-200-2011 and Stanford Cars datasets, respectively. Moreover, in Fig-

Phase	Model layers	Learning rate lr	lr scheduler	Weight decay	Duration
Warm-up	add-on 1×1 convolution prototypical pool	$1.5 \cdot 10^{-3}$ $1.5 \cdot 10^{-3}$	None	None	10 epochs
Joint	convolutions f add-on 1×1 convolution prototypical pool	$5 \cdot 10^{-5}$ $1.5 \cdot 10^{-3}$ $1.5 \cdot 10^{-3}$	by half every 5 epochs	10^{-3}	12 epoch early stopping
After projection	last layer	10^{-4}	None	None	15 epochs

Table 6. Learning schema of the ProtoPool model.

Data	Model	Architecture	Proto. #	Acc [%]
CUB-200-2011	ProtoPool (ours)	DenseNet121	202	73.6 ± 0.4
	ProtoPShare [48]		600	74.7
	ProtoPNet [8]		1476	79.2
	TesNet [57]		2000	84.8 ± 0.2
	ProtoPool (ours)	DenseNet161	202	80.3 ± 0.3
	ProtoPShare [48]		600	76.5
	ProtoPNet [8]		1527	79.9
	TesNet [57]		2000	84.6 ± 0.3
Cars	ProtoPool (ours)	DenseNet121	202	86.4 ± 0.1
	ProtoPShare [48]		980	84.8
	ProtoPNet [8]		2000	86.8 ± 0.1
	TesNet [57]		2000	92.0 ± 0.3

Table 7. Comparison of ProtoPool with other methods based on prototypical parts trained on the CUB-200-2011 and Stanford Cars datasets, considering a various number of prototypes and types of convolutional layers f . One can observe that ProtoPool achieves competitive results, even for models with ten times more prototypes in the case of both datasets. Please note that the results are first sorted by backbone network and then by the number of prototypes.

ures 14 and 16, we present the distribution of values from the prototype assignment matrix for corresponding datasets. As presented, only the ProtoPool model obtains bimodal distribution of 0 and 1, resulting in the binary matrix.

Details on user study questionnaire and results

Each user assessed examples of prototypical parts generated by ProtoPool, ProtoTree [39] and ProtoPool without focal similarity in a randomized way. Naturally, the user does not know which image is generated by which model, and there is no difference in preprocessing those images between models. Each person answered 10 questions for each combination of dataset and model, which resulted in 60 responses per participant. These 60 images were randomly selected from the pool of 180 images (30 for each combination of dataset and model). Each user had unlimited time for the answer. The task was to assign a score from 1 to 5 where 1 meant “I am certain that this is NOT a distinctive feature” and 5 meant “I am sure that this feature is distinctive”. A

sample question is presented in Figure 17 and the results are shown in Table 9. One can observe that ProtoPool achieves the highest number of positive answers (4 and 5). Additionally, all models are generally better for Stanford Cars rather than CUB-200-2011, which can be correlated to the weaker intra-class similarity in the case of car models [39]. Overall, we conclude that enrichment of the model with focal similarity substantially improves the model interpretability, better detecting distinctive features.

Model	Proto. #	Differentiable proto. assignment	Information processing	Reasoning type	Proto. sharing	Class similarity
ProtoPNet	100%	no	simultaneous	positive	none	none
TesNet	100%	no	simultaneous	positive	none	none
ProtoPShare	[20%;50%]	no	simultaneous	positive	direct	direct
ProtoTree	10%	no	successive	positive and negative	indirect	indirect
ProtoPool	10%	yes	simultaneous	positive	direct	direct

Table 8. Comparison of prototypical methods for fine-grained image classification. One can observe that ProtoPool uses only 10% of ProtoPNet’s prototypes, remaining interpretable due to the positive reasoning process. Additionally, ProtoPool, similarly to the ProtoPShare, detects inter-class similarity and shares the prototypes. But, it is trained end-to-end thanks to the differentiable prototypes assignment. On the other hand, ProtoTree is the only model presenting the explanation in a hierarchical way, which requires more time to comprehend according to human cognitive system theory [12].

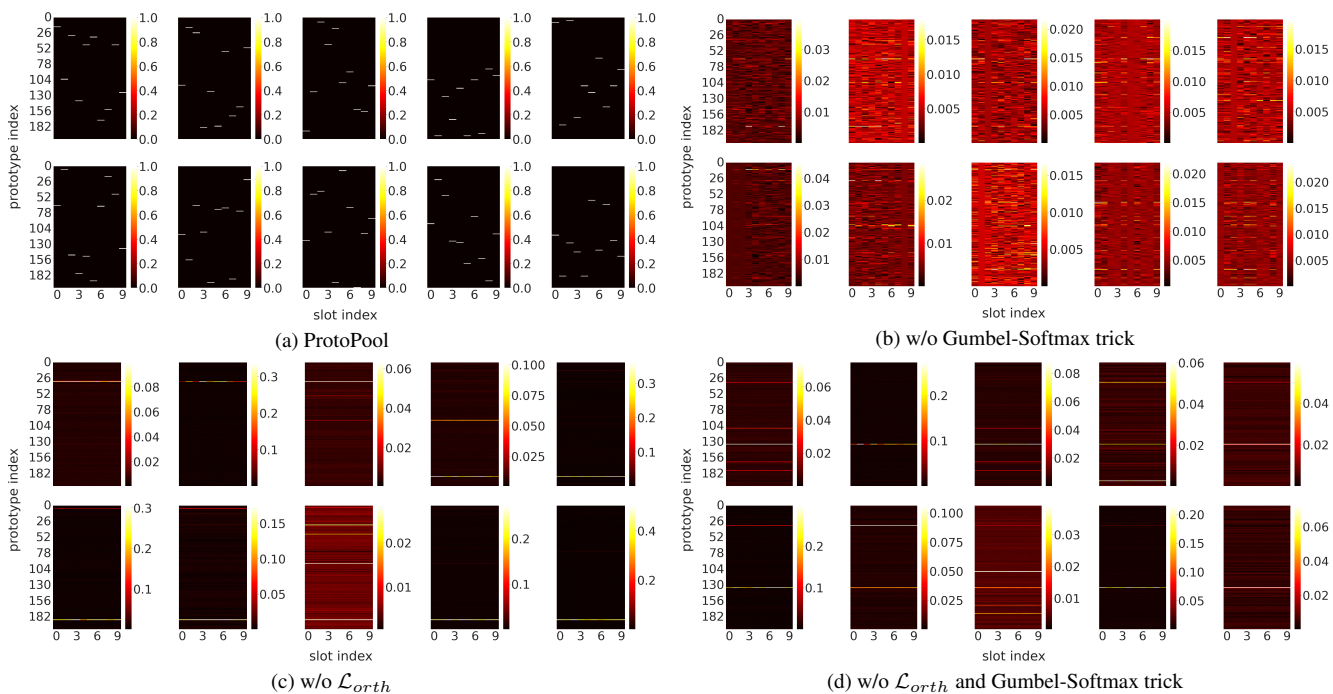


Figure 13. The influence of novel architectural changes on prototypes to slots assignments for ten randomly chosen classes of the CUB-200-2011 dataset. Each class has ten slots (corresponding to columns) to which a prototype (corresponding to rows) can be assigned. As observed, the binarization of the assignment (hard assignment of a prototype) is obtained only for a mix of Gumbel-Softmax and \mathcal{L}_{orth} . Moreover, if one of those factors is missing, the assignment matrix is random or aims to assign the same prototype to all slots. Note that the scale of heatmap colors differs between examples for clarity.

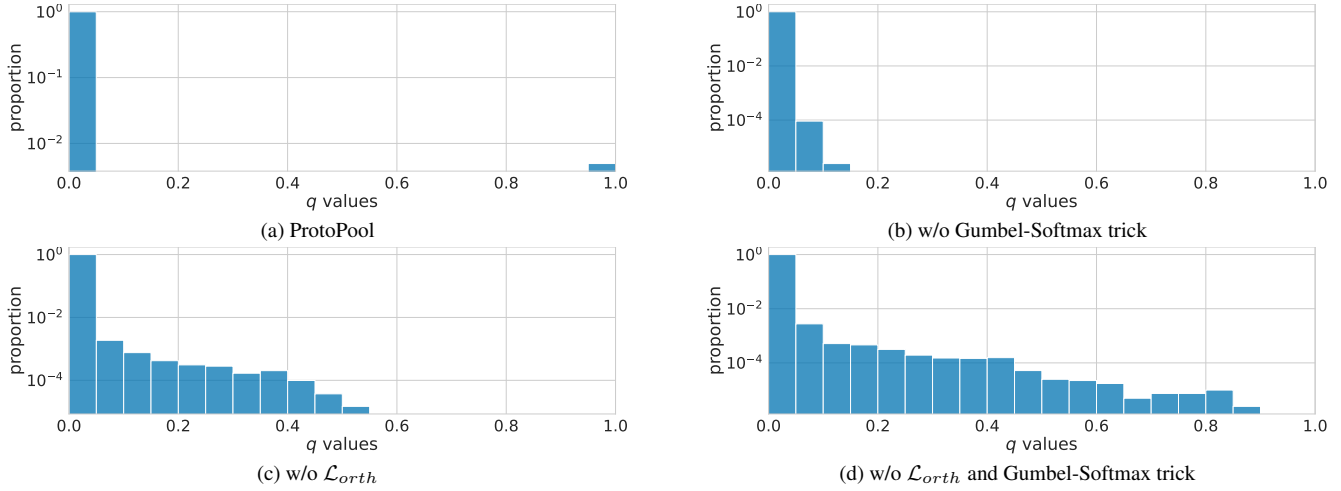


Figure 14. The influence of novel architectural changes on the values of prototypes to slots assignments (q distributions) for the CUB-200-2011 dataset. One can observe that only the ProtoPool model binarizes q distributions. Note that the histograms are in logarithmic scale and normalized.

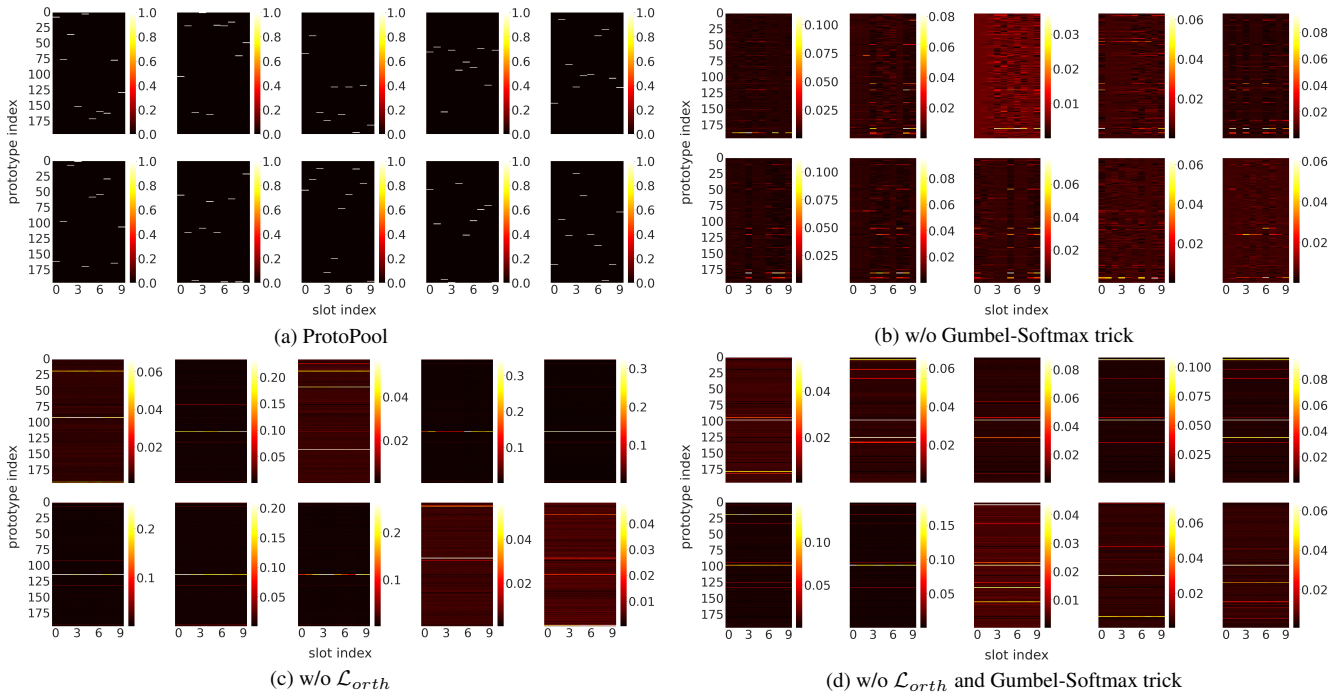


Figure 15. The influence of novel architectural changes on prototypes to slots assignments for ten randomly chosen classes of the Stanford Cars dataset. Each class has ten slots (corresponding to columns) to which a prototype (corresponding to rows) can be assigned. As observed, the binarization of the assignment (hard assignment of a prototype) is obtained only for a mix of Gumbel-Softmax and \mathcal{L}_{orth} . Moreover, if one of those factors is missing, the assignment matrix is random or aims to assign the same prototype to all slots. Note that the scale of heatmap colors differs between examples for clarity.

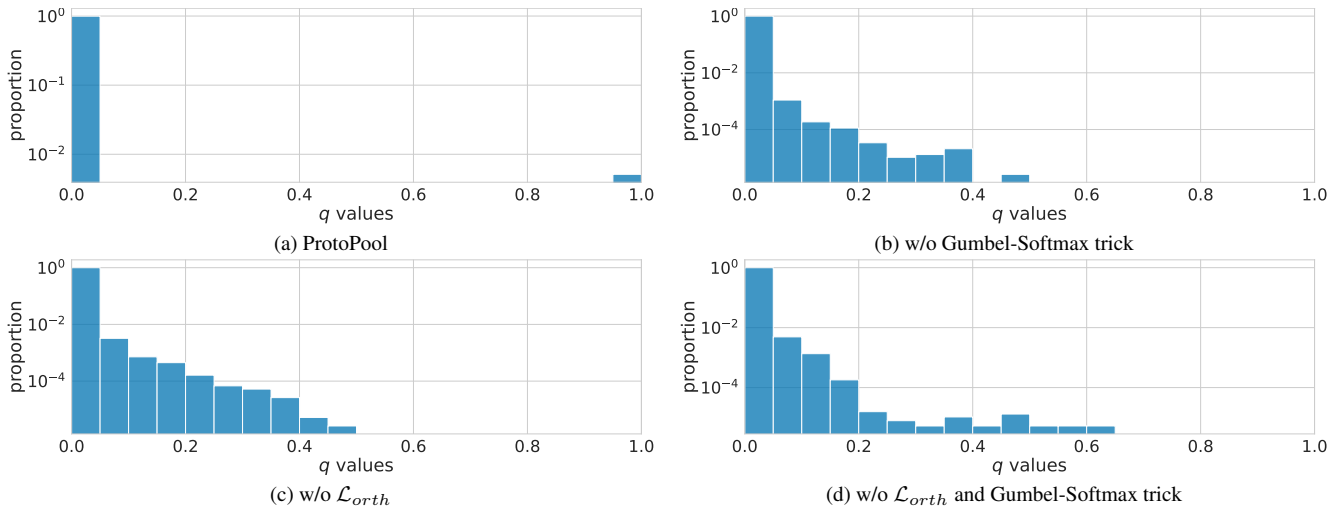
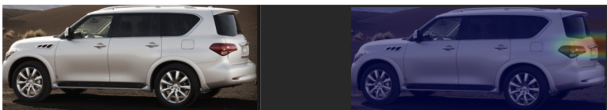


Figure 16. The influence of novel architectural changes on the values of prototypes to slots assignments (q distributions) for the Stanford Cars dataset. One can observe that only the ProtoPool model binarizes q distributions. Note that the histograms are in logarithmic scale and normalized.

Model	Dataset	Answers				
		1	2	3	4	5
ProtoPool	CUB-200-2011	13	27	61	101	98
ProtoTree		180	44	37	23	16
ProtoPool w/o focal similarity		116	61	61	44	18
ProtoPool	Stanford Cars	8	31	50	87	124
ProtoTree		24	56	68	69	83
ProtoPool w/o focal similarity		81	62	65	57	35

Table 9. User study results showing that only ProtoPool has the majority of positive votes (4 and 5) in both datasets. Additionally, ProtoTree is more interpretable for Stanford Cards than for CUB-200-2011.

Is the pointed by the model feature distinctive for the class of a given object?



- 1 - I am certain that this is NOT a distinctive feature
- 2
- 3
- 4
- 5 - I am sure that this feature is distinctive

Figure 17. Sample question from the user study questionnaire.